

Raman spectroscopy of iodine molecules trapped in zeolite crystals

Wenhao Guo, Dingdi Wang, Juanmei Hu, Z. K. Tang,^{a)} and Shengwang Du^{b)}
*Department of Physics, The Hong Kong University of Science and Technology, Clear Water Bay,
 Kowloon, Hong Kong*

(Received 3 November 2010; accepted 8 January 2011; published online 26 January 2011)

We study the Raman spectroscopy of neutral iodine molecules confined in the channels of zeolite $\text{AlPO}_4\text{-5}$ (AFI) and $\text{AlPO}_4\text{-11}$ (AEL) crystals, which shows that the molecular vibration states are significantly modified by the confinements from the nanosize channels. An iodine molecule trapped in the AEL crystal has an effective internuclear potential close to an ideal harmonic oscillator, while that in the AFI crystal behaves similarly to that in free space. The results are further confirmed by measuring the temperature dependence of Raman spectral width. © 2011 American Institute of Physics. [doi:10.1063/1.3549194]

Manipulating and controlling single atoms and molecules confined within a nanosize space not only is of great interest to fundamental research in physics and chemistry, but also may lead to practical applications in nanotechnology and biotechnology.¹⁻³ In the past decade, the nanopore structure of zeolite single crystals has become an important host frame to trap guest atoms and molecules to form many interesting nanostructured systems with extraordinary electro-optical properties. One such example is 0.4 nm single-wall carbon nanotubes formed in the channels of $\text{AlPO}_4\text{-5}$ (AFI) zeolite crystals, which exhibit a surprising superconductivity at 15 K because of the enhanced electron-phonon coupling.⁴⁻⁶ Recently, it was demonstrated that neutral iodine molecules can be loaded into zeolite crystals to form single-molecule wires along the channels.^{7,8} Furthermore, one can also precisely control the spatial orientation of neutral iodine molecules in the elliptical channels of $\text{AlPO}_4\text{-11}$ (AEL) crystals.⁹ But it remains little known how these atoms and molecules interact with the zeolite crystal pore structures.

The electronic structure and energy levels of vibration-rotation states of iodine molecules in free space (FS) have been well studied in the past.¹⁰⁻¹³ Their hyperfine optical transitions¹⁴ have been used to lock a molecular optical clock with higher precision than most rf atomic clocks.¹⁵ However, limited by the vapor pressure, a free-space-based iodine molecular optical clock normally requires a long (~ 1 m) vapor cell.¹⁵ Figure 1(a) shows schematically the vibrational energy and states of an iodine molecule at its ground level in FS. The dashed curve and lines stand for an ideal harmonic oscillator with equally spaced vibrational energy levels. For a large range of internuclear separations, the interaction between the two iodine atoms can be well described by a Morse potential (red solid curve)¹⁶ that results in nonuniformly spaced vibrational states. When an iodine molecule is confined in the nanochannel of a zeolite crystal, these molecular vibrational states will be modified due to the interaction from the channel boundary. Figures 1(b) and 1(c) illustrate an iodine molecule trapped inside the one-dimensional (1D) channel of AFI and AEL crystals, respectively. The

cross section of AFI viewed from the [001] direction is composed of 4-, 6-, and 12-rings. The 12-ring cylindrical channels with a diameter of about 7.3 Å are used to confine iodine molecules, as shown in Fig. 1(b). Removal of a pair of opposing 4-rings converts the 12-rings to an elliptical ring with major and minor diameters of 6.7 and 4.1 Å, respectively, as shown in Fig. 1(c). Obviously, the iodine molecule in the AFI crystal has more freedom than that in AEL where the transverse rotation is frozen.

In this letter, we report the use of Raman optical spectroscopy to study the interaction between the zeolite crystal nanochannels and the confined iodine molecules. Particularly, we are interested in the single-molecule internal vibrational states modified by the surrounding crystal channel wall. From the spectral line shifts and temperature dependence of spectral widths, we find that the iodine molecules trapped in the AEL crystal channels see an effective internuclear potential close to an ideal harmonic oscillator, while those in AFI behave similarly to that in free space but with a minor modification in vibration frequency.

We fabricate AFI and AEL single crystals following the hydrothermal method.^{9,17} Molecular iodine is loaded into the

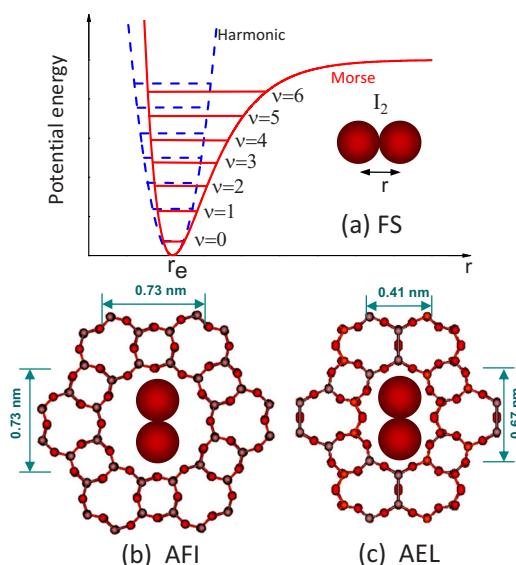


FIG. 1. (Color online) (a) An iodine molecule in FS with a Morse potential. (b) and (c) are an iodine molecule trapped in AFI and AEL crystals, respectively.

^{a)}Electronic mail: phzktang@ust.hk.

^{b)}Author to whom correspondence should be addressed. Electronic mail: dusw@ust.hk.

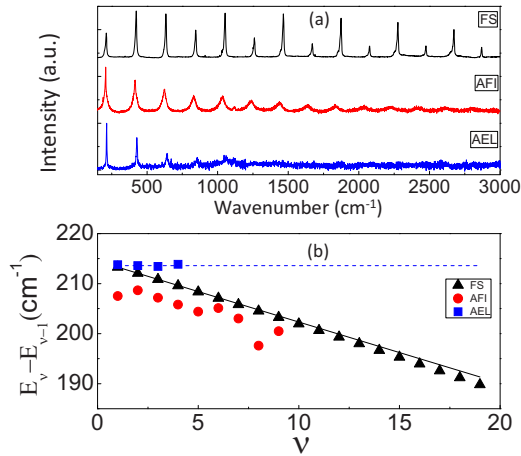


FIG. 2. (Color online) (a) Raman spectra of iodine molecules in FS, AFI, and AEL at $T=30\text{ }^{\circ}\text{C}$. (b) Vibrational energy spacing of iodine molecules vs vibration quantum number ν .

AFI and AEL channels by means of physical diffusion. Initially, the crystals are calcined at $580\text{ }^{\circ}\text{C}$ in O_2 atmosphere for about 24 h to remove the organic templates from the channels. Then the crystals together with a pure iodine source (BDH 99%) are sealed in a Pyrex tube at a vacuum of 10^{-3} mbar. The iodine molecules are diffused into the zeolite channels by physical adsorption. In our experiment, the iodine loading density is so low that the molecular interactions are negligible.

In this work, we focus on the iodine molecules frozen in the transverse direction of the nanochannels. The polarized Raman spectra are measured in a backscattering configuration using a Jobin-Yvon T64000 micro-Raman spectrometer equipped with a liquid N_2 cooled charge-coupled device detector. The linearly polarized excitation laser beam, from an Ar ion laser output at 514.5 nm, has a linewidth of about 6 GHz and a power of 40 mW. The iodine-loaded AFI and AEL crystals are placed in a Linkam Cryostat XY-stage, which can stabilize the sample temperature from $-150\text{ }^{\circ}\text{C}$ to room temperature.

We first compare the Raman spectrum of iodine molecules in FS and in AFI and AEL crystals at room temperature ($T=30\text{ }^{\circ}\text{C}$). In FS, molecular vapor is isotropic and the Raman scattering is polarization independent. For the AFI and AEL cases, the excitation laser beam propagates in the direction perpendicular to the c -axis of the crystal. Especially, in the AEL case, the laser light is polarized along the major axis of the elliptical ring. The experimental spectra are shown in Fig. 2(a). In FS, we detect a few tens of lines that correspond to different vibrational quantum numbers ν , as illustrated in Fig. 1(a). In the AFI and AEL crystals, we resolve nine and four lines, limited by our detector sensitivity and the system noise level. To show the difference in the energy levels caused by the channel confinement, we plot the energy spacing between E_ν and $E_{\nu-1}$ extracted from the Raman spectrum data as a function of the vibrational quantum number ν in Fig. 2(b). As expected, in FS, $E_\nu - E_{\nu-1}$ linearly decreases as ν increases and follows the theoretical (solid black) curve obtained from the Morse potential. For the iodine molecules in the AFI crystal, they follow the similar trend as in FS but with smaller energy spacing. For those in the AEL crystal, the energy spacing is nearly uniform, close to a tighter harmonic oscillator (dashed line) than that in FS.

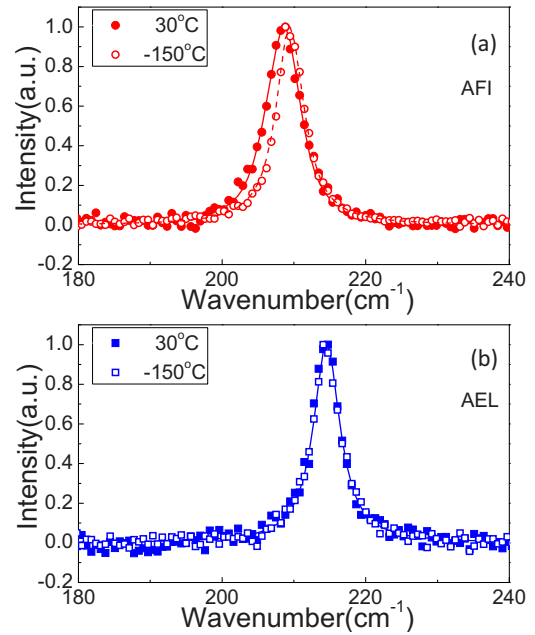


FIG. 3. (Color online) Raman line shape ($\Delta\nu=1$) of iodine molecules in (a) AFI and (b) AEL at different temperatures. The circular and square points are experimental data, and the dashed and solid lines are theoretical curves.

Each Raman spectral line in Fig. 2(a) contains many degenerate lines with equal $\Delta\nu$. For example, the first line corresponds to $\Delta\nu=1$. At a temperature T , the molecules occupy more than one vibrational state with probabilities determined by the Boltzmann distribution

$$\rho_\nu = Q^{-1} e^{-E_\nu/kT}, \quad (1)$$

where Q is the normalization factor and k is the Boltzmann constant. To an ideal 1D harmonic oscillator, the vibrational energies are equally spaced and all Raman transition lines of $\Delta\nu=1$ are degenerate. On the other hand, if the vibrational energies are determined by a Morse-like potential with non-uniform spacing, different Raman transition lines of $\Delta\nu=1$ will not overlap completely. Thus the m th Raman spectral profile (intensity) can be described as

$$I_m(\omega) = \sum_\nu \rho_\nu W_\nu A_{\nu \rightarrow \nu+m}(\omega), \quad (2)$$

where ω is the angular frequency of Raman photon, $A_{\nu \rightarrow \nu+m}(\omega)$ is the normalized line shape function of a transition $\nu \rightarrow \nu+m$, and W_ν is the weight determined by the intrinsic transition strength. The spectral width of the line shape function $A_{\nu \rightarrow \nu+m}(\omega)$ is dominated by the laser linewidth that overwhelms the Doppler broadening effect (<1 GHz). Therefore, we expect that there is no temperature broadening for iodine molecules with an ideal 1D harmonic-oscillator potential. For molecules with a Morse-like potential, however, there will be a significant temperature effect on the spectral width.

Figure 3 shows line shapes of $\Delta\nu=1$ for iodine molecules in the AFI and AEL crystals at two different temperatures. As we increase the temperature from -150 to $30\text{ }^{\circ}\text{C}$, the linewidth of the iodine molecules in the AFI crystal is broadened, while in the AEL crystal we see no detectable change. To calculate the theoretical curves for different temperatures, we obtain the weight W_ν and single-transition line shape function $A(\omega)$ by best fitting to the measured line

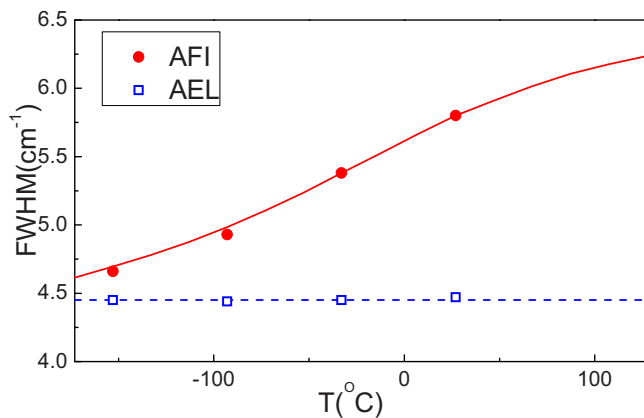


FIG. 4. (Color online) Raman spectral width as a function of temperature for iodine molecules in AFI and AEL crystals. The solid and dashed lines are theoretical curves.

shapes at -150 °C with experimentally determined energy spacing values [dashed curve in Figs. 3(a) and 3(b)]. Then we calculate the line shape at any temperature following Eqs. (1) and (2) without any free parameters. The solid theoretical curve for the AFI case at $T=30$ °C agrees very well with the experimental data. For the AEL case, both dashed and solid curves overlap together and also perfectly match the experiment. Figure 4 shows the full width at half maximum (FWHM) of the line shape as a function of temperature. It is clear that the linewidth of the iodine molecules in the AEL crystal is independent of temperature and agrees well with the ideal 1D harmonic-oscillator model.

In summary, we have studied the Raman spectroscopy of iodine molecules confined in the AFI and AEL nanochannels at different temperatures. The results indicate that the molecular ground vibrational states in the AEL crystal are close to the ideal 1D harmonic oscillator, while in the AFI crystal they are close to that in free space. Our work shows that the optical spectroscopy is an efficient way to study molecular

interaction at nanoscale. Besides the weak interaction from the host crystal, these iodine molecules are isolated from each other and can have much high density than those in free space at room temperature. A zeolite single crystal (with a dimension of about 100 μm) filled by iodine molecules may be used for molecular optical clock¹⁵ with a dramatic reduction in the device size. It may also find application in molecule-based quantum information processing.¹⁸

The work was supported by the Hong Kong Research Grants Council under the Grant No. 604210.

- ¹L. D. Gelb, K. E. Gubbins, R. Radhakrishnan, and M. Sliwinski-Bartkowiak, *Rep. Prog. Phys.* **62**, 1573 (1999).
- ²G. Hummer, J. C. Rasaiah, and J. P. Noworyta, *Nature (London)* **414**, 188 (2001).
- ³P. Xiu, B. Zhou, W. Qi, H. Lu, Y. Tu, and H. Fang, *J. Am. Chem. Soc.* **131**, 2840 (2009).
- ⁴N. Wang, Z. K. Tang, G. D. Li, and J. S. Li, *Nature (London)* **408**, 50 (2000).
- ⁵Z. K. Tang, L. Y. Zhang, N. Wang, X. X. Zhang, G. H. Wen, G. D. Li, J. N. Wang, C. T. Chan, and P. Sheng, *Science* **292**, 2462 (2001).
- ⁶R. Lortz, Q. Zhang, W. Shi, J. T. Ye, C. Qiu, Z. Wang, H. He, P. Sheng, T. Qian, Z. Tang, N. Wang, X. Zhang, J. Wang, and C. T. Chan, *Proc. Natl. Acad. Sci. U.S.A.* **106**, 7299 (2009).
- ⁷F. Y. Jiang and R. C. Liu, *J. Phys. Chem. Solids* **68**, 1552 (2007).
- ⁸J. T. Ye, Z. K. Tang, and G. G. Siu, *Appl. Phys. Lett.* **88**, 073114 (2006).
- ⁹J. P. Zhai, I. L. Li, S. C. Ruan, H. F. Lee, and Z. K. Tang, *Appl. Phys. Lett.* **92**, 043117 (2008).
- ¹⁰W. Kiefer and H. J. Bernstein, *J. Mol. Spectrosc.* **43**, 366 (1972).
- ¹¹W.-Y. Cheng, L. Chen, T. H. Yoon, J. L. Hall, and J. Ye, *Opt. Lett.* **27**, 571 (2002).
- ¹²L. Chen, W.-Y. Cheng, and J. Ye, *J. Opt. Soc. Am. B* **21**, 820 (2004).
- ¹³L. Chen, W. A. de Jong, and J. Ye, *J. Opt. Soc. Am. B* **22**, 951 (2005).
- ¹⁴P. Jungner, S. Swartz, M. Eickhoff, J. Ye, J. L. Hall, and S. Waltman, *IEEE Trans. Instrum. Meas.* **44**, 151 (1995).
- ¹⁵J. Ye, L. S. Ma, and J. L. Hall, *Phys. Rev. Lett.* **87**, 270801 (2001).
- ¹⁶P. M. Morse, *Phys. Rev.* **34**, 57 (1929).
- ¹⁷F. Y. Jiang, J. P. Zhai, J. T. Ye, J. R. Han, and Z. K. Tang, *J. Cryst. Growth* **283**, 108 (2005).
- ¹⁸K. Hosaka, H. Shimada, H. Chiba, H. Katsuki, Y. Teranishi, Y. Ohtsuki, and K. Ohmori, *Phys. Rev. Lett.* **104**, 180501 (2010).